Chirped Gaussian Pulse excitation of a harmonic oscillator

R. A. Alharbey,[1,*] H. Gasim,[1] F. N. M. Al-Showaikh,[2] and S. S. Hassan[2]

[1] *King Abdulaziz University, Faculty of Science,*

Mathematics Department P. O. Box 42696, Jeddah 21551, Kingdom of Saudi Arabia

[2] *University of Bahrain, College of Science, Mathematics Department, P. O. Box 32038, Kingdom of Bahrain*

[*] Corresponding author email: rania.math@gmail.com

We investigate the basic problem of the interaction of a single quantised mode of the radiation field, modelled as quantised harmonic oscillator (HO) with a laser pulse of chirped Gaussian line-shape. The average photon number and the transient emitted spectrum are calculated analytically in terms of the error function of complex argument. The spectral peaks of the line structure of the emitted radiation are examined for different system parameters and initial states of the HO.

1.. INTRODUCTION

The field of quantum optics is concerned with quantum properties of radiation-matter and radiation -radiation interaction. The simplest model of matter is a single atom of 2-level structure, whilst the simplest wave radiation is modelled as a simple harmonic oscillator (HO).

The model of a laser pulsed- driven- single quantised HO has been examined previously for different shapes of laser pulses. Specifically, the Fourier transform (FT) transient scattered spectrum of the HO was studied in the case of multi-mode rectangular pulse [1] and both the FT and wavelet spectra were studied in the case of sin^2-pulse shape [2-4].

In addition to its fundamental interest, HO represents two limiting cases: a large (infinite) number of Rydberg atoms in contact with thermal [5] or squeezed vacuum [6] reservoirs. Here, we extend the above investigation (HO $\oplus$ pulsed laser) to the case of a chirped Gaussian laser pulse.

The paper is presented as follows: in sec 2, we present the corresponding Heisenberg equations of motion and their solutions in the case of chirped Gaussian pulse. In sec 3 and 4 we calculate and examine computationally the average photon number and the scattered spectrum of the HO, respectively. A summary is given in sec 5.

2.. THE MODEL EQUATIONS

(a) Exact solutions

The Hamiltonian model representing the interaction of a single quantised (non-dissipative) HO with a (classical) laser pulse within the RWA is of the following form [2] (in units of $\hbar = 1$);

$$H = \omega_0 \hat{a}^\dagger \hat{a} + \Omega_o (f(t)\hat{a}^\dagger e^{-i\omega_L t} + f^*(t)\hat{a} e^{i\omega_L t}) \tag{1}$$

where ω_0 is the HO frequency, ω_L is the oscillating frequency of the pulse envelope, $f(t)$ is the pulse

shape function and Ω_0 is the pulse strength (Rabi frequency).

The first term of the Hamiltonian (1) is the unperturbed Hamiltonian of the HO, while the rest of terms represent the interaction Hamiltonian between the HO and the driving pulse.

Heisenberg equations of motion for the operators $\hat{a}$ and $\hat{a}^\dagger$ according to the Hamiltonian (1) are of the form,

$$\begin{aligned} \dot{\hat{a}} &= -i\omega_o\hat{a} - i\Omega_o f(t)e^{-i\omega_L t} \\ \dot{\hat{a}}^\dagger &= i\omega_o\hat{a}^\dagger + i\Omega_o f^*(t)e^{i\omega_L t} \end{aligned} \tag{2}$$

The formal operator solutions of (2) for arbitrary pulse shape $f(t)$ are given by ,

$$\begin{aligned} \hat{a}(t) &= \hat{a}(t_o)e^{-i\omega_o t} - i\Omega_o e^{-i\omega_o t}\int_{t_o}^{t} f(t')e^{-i\Delta t'}dt' \\ &= e^{-i\omega_o t}\hat{A}(t). \end{aligned} \tag{3a}$$

$$\hat{a}^\dagger(t) = e^{i\omega_o t}\hat{A}^\dagger(t) \tag{3b}$$

where,

$$\hat{A}(t) = \hat{a}(t_o) - i\Omega_o I(t) \tag{4}$$

$$I(t) = \int_{t_o}^{t} f(t')e^{-i\Delta t'}dt' \tag{5}$$

and $\Delta = (\omega_L - \omega_o)$ is the frequency detuning parameter, and t_o is the initial time (which depends on the switching of the pulse).

(b) Case of chirped Gaussian pulse.

The pulse shape in this case takes the form ,

$$f(t) = e^{-(1+ic)(\frac{t}{\tau_o})^2} \tag{6}$$

Where C is the chirp parameter, τ_o is the $\frac{1}{2}$-width of the pulse. For $C \neq 0$, $f(t)$ has the complex

form,

$$f(\tau) = f_r(\tau) + i f_i(\tau);\ \tau = \frac{t}{\tau_o} \tag{7a}$$

Where,

$$f_r(\tau) = e^{-\tau^2} cos(c\tau^2) \tag{7b}$$

$$f_i(\tau) = e^{-\tau^2} sin(c\tau^2) \tag{7c}$$

Effect of the chirp parameter to stretch the pulse τ in an oscillatory pattern-as seen in Fig.1a at fixed values of $C = \pm 2$ and in Fig.1b for larger $C = \pm 6$. Increasing the value of $C = 6$ induces wave oscillations, while the negative value of (C) is to change the phase of the oscillations in the imaginary part function $f_i(t)$, as seen in the insets of Fig.1a,b. For fixed values of τ, both $f_r(C), f_i(C)$ are purely sinusoidal functions of C.

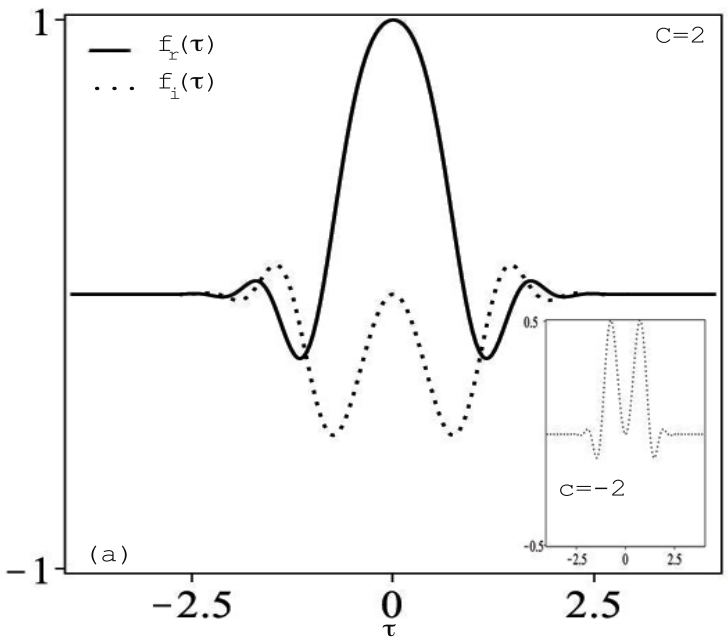

Fig.1a: *The real and the imaginary parts of $f_r(\tau), f_i(\tau)$ against (τ) at fixed value of $C = 2$.. Inset shows $f_i(\tau)$ for $c = -2$*

Now, due to the *smooth* switch-on of the Gaussian pulse we take $t_o \to -\infty$ (unlike the sharp switch-on of other pulses, like rectangular, at $t_o = 0$). Thus, the expression for $I(t), eq(5)$ with $f(t)$ given by (6) is

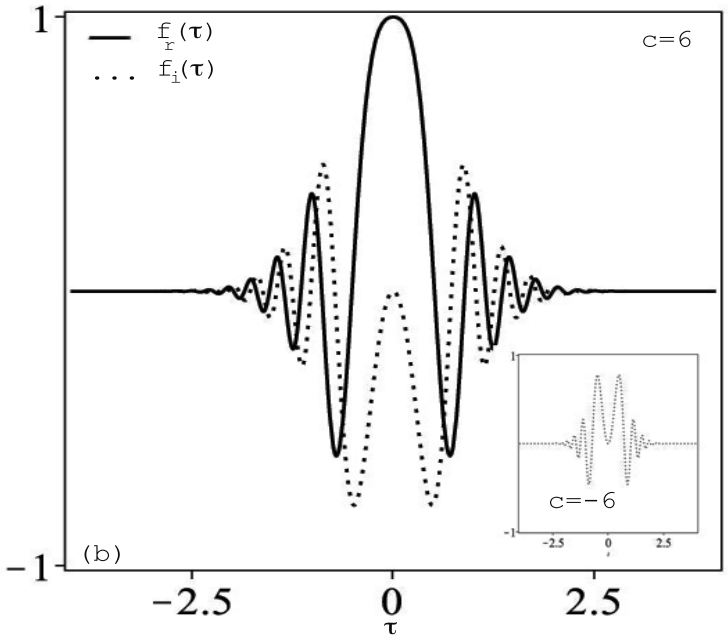

Fig.1b: *As Fig.1a but for* $C = 6$.

expressed in terms of the error function erf (z) of complex argument,

$$I(t) = \int_{-\infty}^{t} f(t')e^{-i\Delta t'}dt' \tag{8a}$$

$$= \frac{\tau_o\sqrt{\pi}}{2\sqrt{a}}e^{\frac{b^2}{a}}(\text{erf}\,(C_1t + C_2) + 1) \tag{8b}$$

where $a = 1 + iC$, $b = \frac{i\Delta\tau_o}{2}$, $C_1 = \dfrac{\sqrt{a^*}}{\tau_o}$, $C_2 = \dfrac{b^*}{\sqrt{a^*}}$ and the error function erf $(z) = \frac{2}{\sqrt{\pi}}\int_0^z e^{-t^2}dt$.(see, e.g.[7]).

3.. AVERAGE PHOTON NUMBER

The HO photon number operator $\hat{n}(t) \equiv \hat{a}^\dagger(t)\hat{a}(t)$ using $eq(3)$ is given by,

$$\hat{n}(t) = \hat{a}^\dagger(t_o)\hat{a}(t_o) + \Omega_o^2|I(t)|^2 - i\Omega_o\hat{a}^\dagger(t_o)I(t) + i\Omega_o\hat{a}(t_o)I^*(t) \tag{9}$$

Where, I(t) is given by (8) with $t_o = -\infty$. The averaged photon number $\bar{n}(t) = \langle \hat{n}(t) \rangle$ of the HO, in the general case of initial coherent state $|\alpha\rangle$ is given by,

$$\bar{n}_\alpha(t) = \langle \alpha | \hat{a}^\dagger(t_o)\hat{a}(t_o)|\alpha\rangle + \Omega_o^2 |I(t)|^2 - i\Omega_o(\langle \alpha|\hat{a}^\dagger(t_o)|\alpha\rangle I(t) - c.c.) \tag{10}$$

$$= |\alpha|^2 + \Omega_o^2 |I(t)|^2 + 2\Omega_o Im(\alpha^* I(t)) \tag{10a}$$

The first term in (10) represents the initial average photon number of the HO $\langle \hat{a}^\dagger(t_o)\hat{a}(t_o)\rangle = |\alpha|^2$, while the second term in Ω_o^2 represents the intensity of the (classical) pulse. The last term represents the change in the photon number $\bar{n}(t)$ due to the exchange of initial amplitude $< \hat{a}^\dagger(t_o) >= \alpha^*$ of the HO with the driving pulse.

Two special cases of initial state for the HO are:

(i) The zero (vacuum) number state $|0\rangle$, $\langle \hat{a}^\dagger(t_o)\hat{a}(t_o)\rangle = 0$, $\langle \hat{a}^\dagger(t_o)\rangle = 0$, and (10a) reduced to ,

$$\hat{n}_o(t) = \Omega_0^2 |I(t)|^2. \tag{10b}$$

(ii) In the number state $|n\rangle$ $(n \neq 0)$, $\langle \hat{a}^\dagger(t_o)\hat{a}(t_o)\rangle = n_o$, $\langle \hat{a}^\dagger(t_o)\rangle = 0$, and (10a) reduced to,

$$\bar{n}_{n_o}(t) = n_o + \Omega_o^2 |I(t)|^2 \tag{10c}$$

The computational of plots of the normalised average photon numbers $\bar{n}_o(t), \bar{n}_{n_o}(t), \bar{n}_\alpha(t)$, $eqs(10b, c, a)$, are shown in fig(2-4).

(i) Initial vacuum state.

At exact resonance ($\Delta = 0$) and for $C = 0$, Fig.2a shows that the normalized average photon number $\bar{n}_o(\tau)$ is independent of the pulse strength Ω_o^2 and reaches its stationary maximum value monotonically around the normalised time $\tau = 2$. For non-zero chirp $|C| = 10$, the reach to a lesser value of the steady state is oscillatory within the period $(0, 2)$. In the off resonance case ($\Delta' = \Delta\tau_o = 4$) and $C = 0$, Fig.2b shows that $n_o(\tau)$ has essentially a Gaussian profile. For $\tau > 0$ and positive $C = 4$, the amplitude of oscillations is reduced, while for negative $C = -4$, the approach to the steady value is much less oscillatory. For Δ, C of the same (opposite) sign the results are the same as the full (dotted) lines.The steady state value is less

reduced for $C = 4$ compared with negative $C = -4$.

(ii) Initial number state , $n_o = 1, \Omega'_o = 10$.

In the resonance case ($\Delta = 0$) and $C = 0$, Fig.3a shows that the normalised average photon number $\bar{n}_{n_o}(\tau)$ has a monotonic behaviour similar to Fig.2a of the vacuum state. For non-zero positive chirp, $\bar{n}_{n_o}(\tau)$ has a peak around $\tau = 0$ with prominent oscillations for $\tau > 0$, while for negative chirping reduced oscillations show only for $\tau > 0$. For $\Delta = 4$ and $C = 0$, the profile shown in Fig.3b is a main peak at $\tau = 0$ with two small symmetrical side peaks. With positive $C = 4$, the small peak for $\tau < 0$ is flattened while the peak for $\tau > 0$ switches to a decaying oscillatory pattern. For $C = -4$, there is dimensioning two peaks for $\tau < 0$, while for $\tau > 0$ the approach to the long time value is much less oscillatory, compared with the positive $C = 4$. For $\Delta = -4$, the full ($C = 4$) and the dotted ($C = -4$) lines are exchanged.

(iii) Initial coherent state , $\alpha = 5$, $\Omega'_o = 10$.

For real amplitude ($\theta = 0$) of the coherent parameter α and at exact resonance $\Delta = 0$, Fig.4a, shows that the monotonic profile of the normalized average photon number $\bar{n}_\alpha(\tau)$ in the case $C = 0$ turns to asymmetric oscillatory behaviour with respect to $\tau = 0$ for positive C. For negative C we have the same behaviour but with a lesser amplitude of oscillations. In the off-resonance case ($\Delta = 4$) and $C = 0$ the profile shown in Fig.4b has the shape of "Mexican hat". This turns for $C = 4$ to oscillatory behaviour for $\tau > 0$ and fading oscillation for $\tau < 0$. The opposite behaviour is obtained for $C = -4$. For $\Delta = -4$ and $C = 0$, the profile shown in Fig.4c is an inverted Mexican hat which turns to asymmetric profile for $C = 4$ with decaying oscillatory for $\tau < 0$ and much reduced oscillation for $\tau > 0$ .The behaviour for $\tau \lessgtr 0$ is reversed for $C = -4$.

In all the above three initial states of HO, similar signs for (C, Δ) leads to a lesser steady value of $n(\tau)$, as compared with opposite signs of (C, Δ).

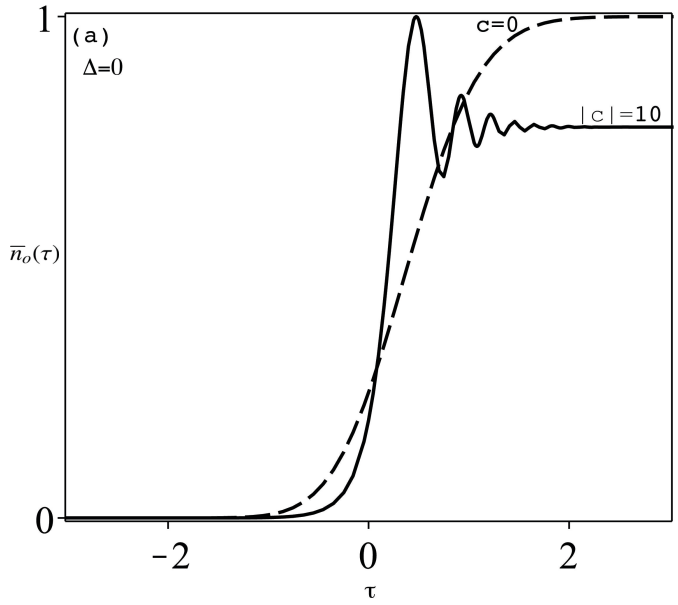

Fig.2a: *Normalised average photon number for* $\bar{n}_o(\tau) = \langle \bar{n}(\tau) \rangle / \langle \bar{n}(\tau) \rangle_{max}$ *for the initial vacuum state at* $\Delta' = 0$ *and for* $|C| = 0, 10$.

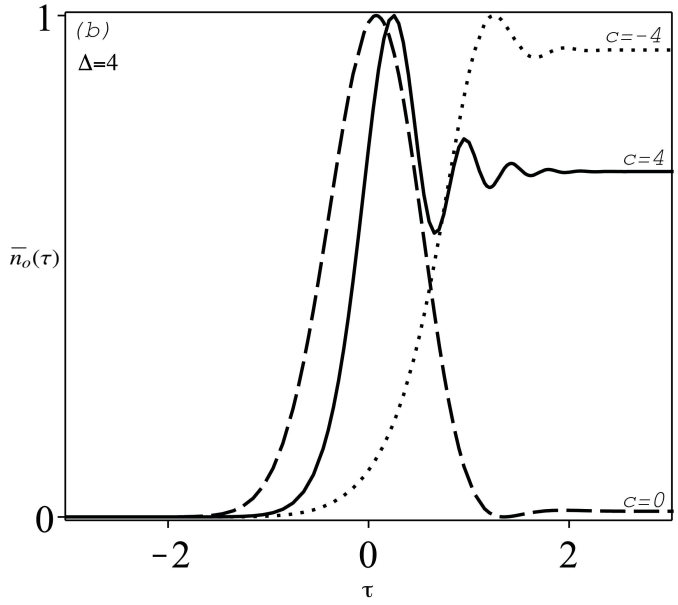

Fig.2b: *Same as Fig.2a but for* $\Delta' = 4$ *and* $C = 0, \pm 4$.

4.. TRANSIENT SCATTERED SPECTRUM

Information about the scattered radiation due to the interaction of the HO with the driving pulse is achieved through the transient spectrum function. This is given by (e.g.[2]),

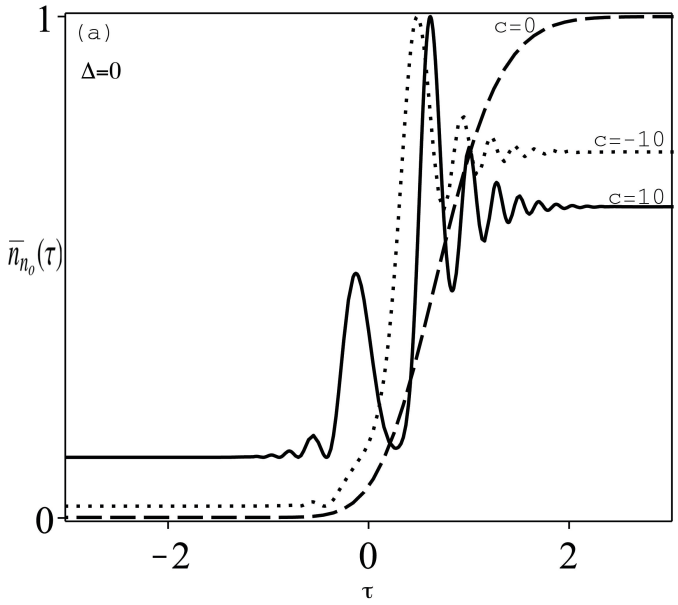

Fig.3a: *. The same as Fig.2a but for $\bar{n}_{n_o}(\tau)$ in the initial number state with $n_o = 1, \Omega'_o = 10, |C| = 0, 10, \Delta' = 0$*

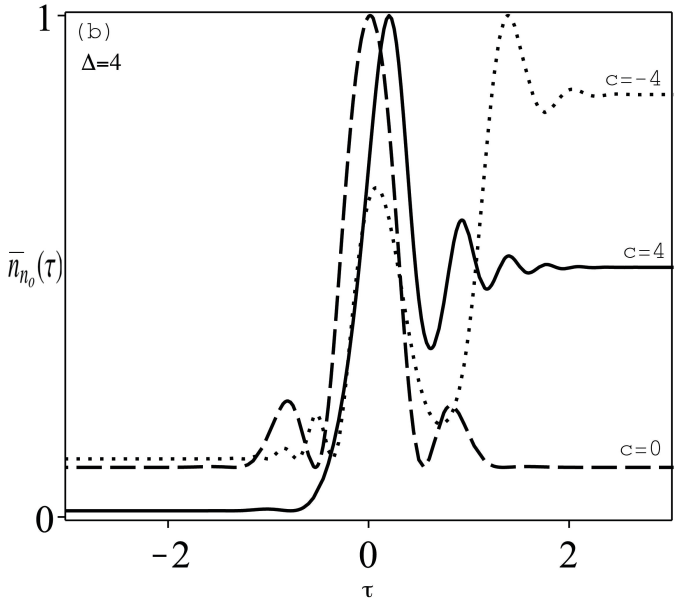

Fig.3b: *Same as Fig.2b but for the initial number state n_o and for $\Delta' = 4, C = 0, \pm 4$.*

$$S(t, D, \Gamma) = 2\Gamma \int_{-\infty}^{t} dt_1 \int_{-\infty}^{t} dt_2 e^{(-\Gamma+iD)(t-t_1)} e^{(-\Gamma-iD)(t-t_2)} \langle \hat{A}^\dagger(t_1)\hat{A}(t_2)\rangle \tag{11}$$

where $D = \omega - \omega_0$ is the frequency mismatch between the frequency (ω) of the instrument (photon detector) and the HO frequency (ω_o), and Γ is the detector's width. The function $\langle \hat{A}^\dagger(t_1)\hat{A}(t_2)\rangle$, with $\hat{A}(t)$

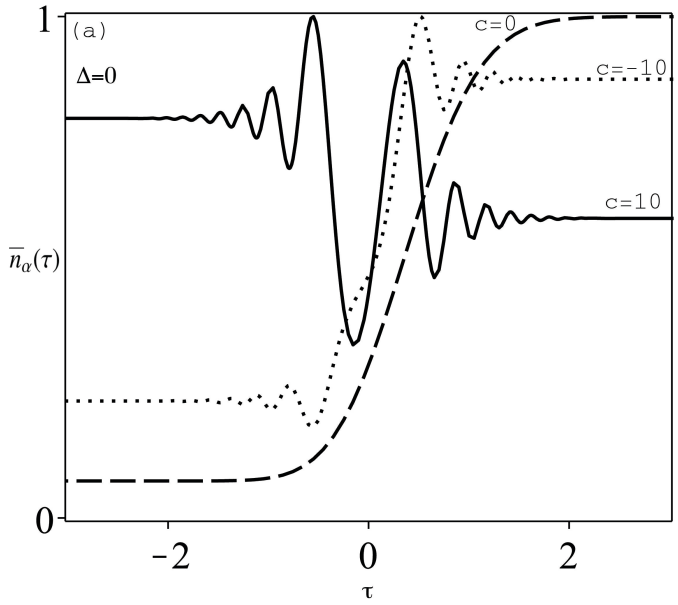

Fig4a: *Same as Fig.2a but for* $\bar{n}_\alpha(\tau)$ *in the initial coherent state with* $\theta = 0, \alpha = 5, \Omega'_o = 10$

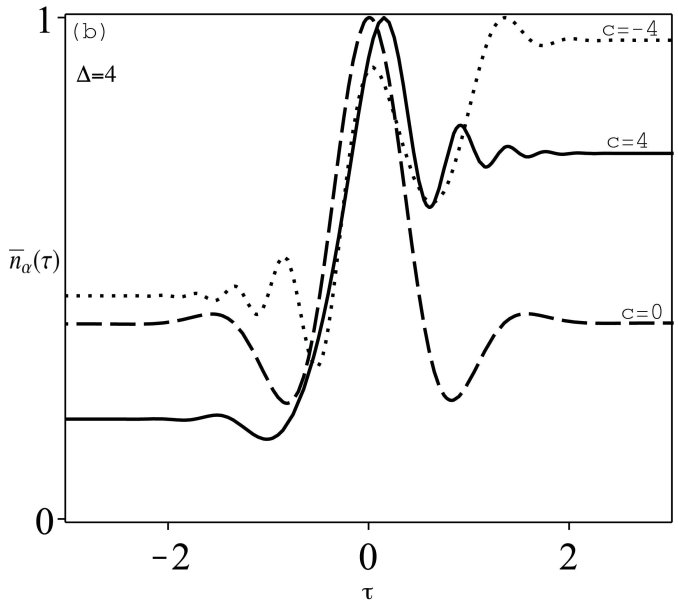

Fig.4b: *Same as Fig.4a but with* $\Delta' = 4, C = 0, \pm 4$

given by (4) and (5), is the auto-correlation function for the shift (creation and annihilation) operators. From (4) and its conjugated, we have

$$\langle \hat{A}^\dagger(t_1)\hat{A}(t_2)\rangle = \langle \hat{a}^\dagger(t_o)\hat{a}(t_o)\rangle + \Omega_o^2 I^*(t_1)I(t_2) - i\Omega_o\langle \hat{a}^\dagger(t_o)I(t_2)\rangle + i\Omega_o\langle \hat{a}(t_o)I^*(t_1)\rangle \tag{12}$$

Where $I(t)$ is given by (8).

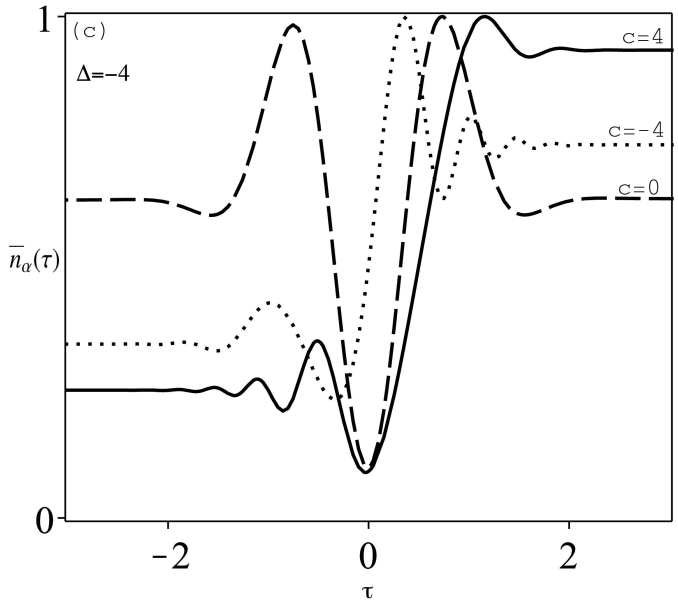

Fig.4c: *Same as Fig.4a but with* $\Delta' = -4, C = 0, \pm 4$

Inserting (12) into (11), we have the following form for the spectrum,

$$S(t, D, \Gamma) = 2\Gamma e^{-2\Gamma t}[n(t_o)|J_1(t)|^2 + \Omega_o^2|J_2(t)|^2 - 2\Omega_o Im(\bar{a}(0)J_1^*(t)J_2(t))] \tag{13}$$

where, $\bar{n}(t_o) = \langle a^\dagger(t_o)a(t_o)\rangle, \bar{a}(t_o) = \langle \hat{a}(t_o)\rangle$, and the quantities $J_{1,2}(t)$ are given by,

$$J_1(t) = \int_{-\infty}^{t} e^{(\Gamma - iD)t'}dt' = \frac{e^{(\Gamma - iD)t}}{\Gamma - iD}. \tag{14a}$$

$$J_2(t) = \int_{-\infty}^{t} e^{(\Gamma_1 - iD)t'} I^*(t')dt' \tag{14b}$$

$$= \frac{\tau_o}{2}\sqrt{\frac{\pi}{a^*}}e^{\frac{b^2}{a^*}} \int_{-\infty}^{t} \left(\text{erf}\,(\sqrt{a}\frac{t'}{\tau_o} + \frac{b}{\sqrt{a}}) + 1\right) e^{-(\Gamma - iD)t'}dt'$$

$$= \frac{\tau_o\sqrt{\pi}}{2\sqrt{a^*}}e^{\frac{b^2}{a^*}}(A_1(t) - J_1(t)) \tag{15a}$$

Where,

$$A_1(t) = \frac{1}{\Gamma - iD}e^{-dC_2}\left[e^{dC_2}e^{(\Gamma - iD)t}\text{erf}\,(C_1 t + C_2) - e^{\frac{d^2}{4}}(\text{erf}\,(c_1 t + c_2 - \frac{d}{2}) + 1)\right] \tag{15b}$$

With, $d = \dfrac{\Gamma - iD}{C_1}$, $C_{1,2}, a, b$ are given below eq.(8b).

Effect of pulse shape, through $I^*(t)$ in $J_2(t)$, is shown in the last two terms in (13), While the first term

is only associated with the initial average photon number, $\bar{n}(t_o)$, of the HO.

We consider the three cases of initial conditions of the HO.

(a) The HO is initially in the zero (vacuum) number state $|0\rangle, \bar{n}(t_o) = 0, \bar{a}(t_o) = 0$, so (13) is reduced to,

$$S_o(t, D, \Gamma) = 2\Gamma\Omega_o^2 e^{-2\Gamma t}|J_2(t)|^2 \tag{16a}$$

(b) The HO is initially in the number state $|n\rangle (n \neq 0)$,

$\bar{n}(t_o) = n_o, \bar{a}(t_o) = 0$, and (13) is reduced to ,

$$S_{n_o}(t, D, \Gamma) = 2\Gamma e^{-2\Gamma t}(n_o|J_1(t)|^2 + \Omega_o^2|J_2(t)|^2) \tag{16b}$$

(c) The HO is initially in the coherent state $|\alpha\rangle$, $\bar{n}(t_o) = |\alpha|^2, \bar{a}(t_o) = \alpha$, and (13) is of the general form,

$$S_\alpha(t, D, \Gamma) = 2\Gamma e^{-2\Gamma t}[|\alpha|^2|_1(t)|^2 + \Omega_o^2|J_2(t)|^2 - 2\Omega_o Im(\alpha J_1^*(t)J_2(t))] \tag{16c}$$

The computational plots of the normalised spectra $S_{o,n_o,\alpha}(D') = \dfrac{S_{o,n_o,\alpha}(t, D, \Gamma)}{\max(S(t, D, \Gamma))}$, eqs(16), are shown in the following Figs.(5-7).

(i): Initial vacuum state

For observation time $\tau = 0.7\pi$ and for pulse $\frac{1}{2}$-width $\tau_o' = 0.4, C = 0$ and increasing detuning $\Delta' = 0, 9, 15$, the normalised spectrum $S_o(D')$ in Fig.5a shows that the symmetric single peak at $D' = 0$ has asymmetric structure, which, with larger Δ' it develops to a broader peak at $D' \simeq \Delta'$. For non-zero $|C| = 1$ and for larger $\Delta' = 15$, Fig.5b show that the central Lorenzian at $D' = 0$ is accompanied with enhanced oscillation of larger amplitude for positive C, compared with negative C.These oscillations disappear for larger $|C| = 3$.

(ii): Initial number state

The effect of the initial number state ($n_o = 1$) on the normalised spectrum $S_{n_o}(D')$ is best seen in Fig.6 for $\Omega_o \gg n_o$, $C = 5$. For early observation, $\tau = 0.1\pi$ and pulse $\frac{1}{2}$-width $\tau_o' = 1$, the spectrum has a distorted broader peak and flattened top to the left (right) of $D' = 0$ for $C \gtrless 0$, respectively. With increased detuning Δ', the central Lorentzian structure at $D' = 0$ gets narrower with fading oscillations due to the chirp parameter, $C \neq 0$.

(iii): Initial coherent state

For observation time $\tau' = 0.3\pi$ and $\tau'_o = 0.3$, the normalised spectrum with the initial coherent state $S_\alpha(D')$ in Fig.7 shows that in the off-resonance case ($\Delta' \neq 0$) there is an asymmetric hole burning structure that depends on the sign of the chirp parameter C.

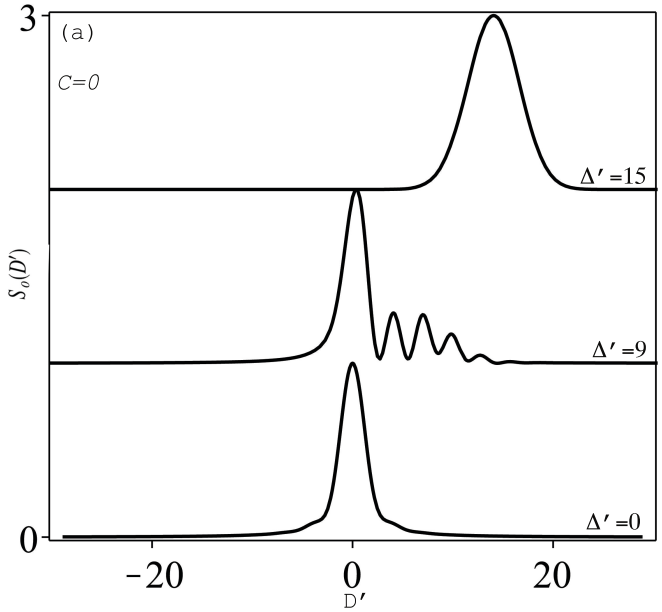

Fig5a: *The normalised spectrum $S_o(D')$ in the initial vacuum state for $\tau = 0.7\pi, \tau'_o = 0.4, c = 0$ and different $\Delta' = 0, 9, 15$.*

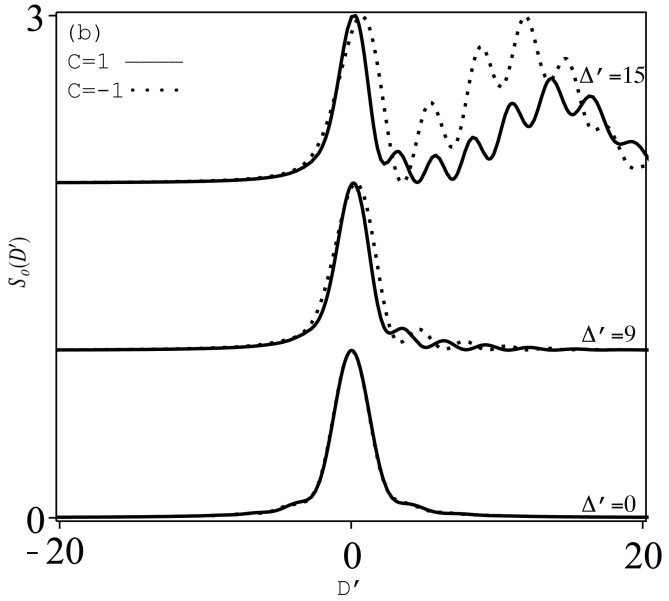

Fig5b: *Same as Fig.5a but for $C = 1, -1$.*

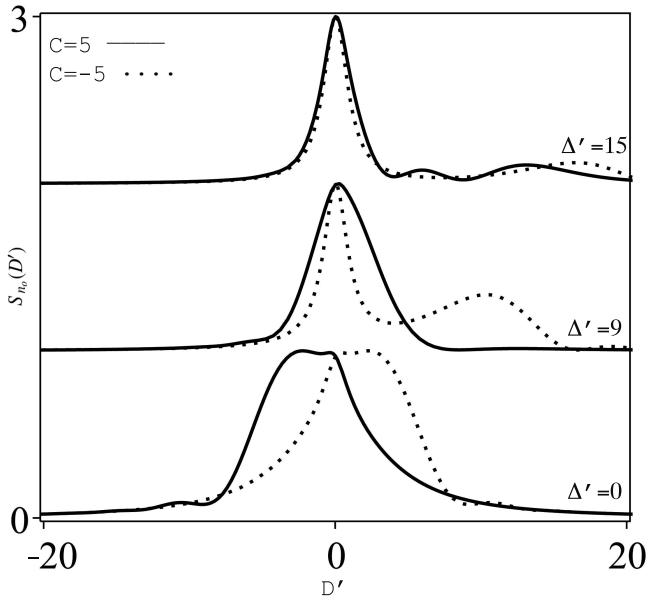

Fig6: *The normalised spectrum* $S_{n_o}(D')$ *in the initial number state for* $\tau = 0.1\pi, \tau_o' = 1, |C| = 5, n_o = 1, \Omega' = 10$ *and different* $\Delta' = 0, 9, 15$.

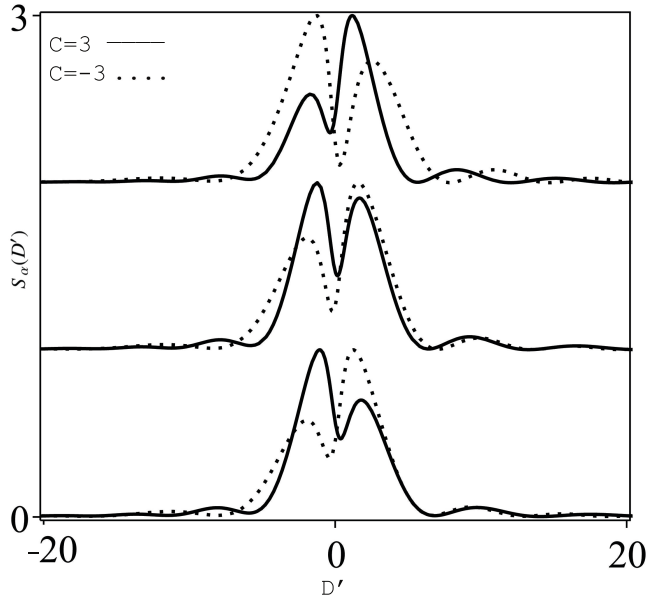

Fig7: *The normalised spectrum* $S_\alpha(D')$ *in the initial coherent state for* $\tau = 0.3\pi, |\Delta'| = 5, 8, 12, \tau_o = 0.3, \alpha = 1, \theta = 0.5\pi, |C| = 3$.

5.. CONCLUSION

The model of a single quantized harmonic oscillator (HO) coupled with a single chirped Gaussian laser pulse is examined analytically and computationally. This concerns:

(i) The average photon number $\bar{n}(t)$ of the HO (related to its energy), and

(ii) The transient scattered radiation spectrum $S(t, D, \Gamma)$.

Exact expressions of $\bar{n}(t)$, $S(t, D, \Gamma)$ are obtained in terms of the error function of complex argument and for arbitrary initial state of the HO. The system parameters (pulse strength, frequency detuning, chirp parameter, initial HO state) induce asymmetry and oscillatory structure in the spectrum.

Further work may generalise the present model to the following cases:

(a) A train of chirped Gaussian laser pulses, where the combined effect of repetition period between pulses and the chirped parameter introduce an additional control parameter,

(b) The case of anharmonic oscillator, as realised in Josephson device [8], where available giant nonlinearity parameter [9] may further cause asymmetry in the scattered spectrum.

REFERENCES

[1] A. Joshi and S. S. Hassan, Resonance fluorescence spectra of a two-level atom and of a harmonic oscillator with multimode rectangular laser pulses, *J. Phys. B: At. Mol. Opt. Phys.* **35** (2002) 1985-2003.

[2] S. S. Hassan, R. A. Alharbey and H. Al-Zaki, Transient spectrum of $\sin^2$-pulsed driven harmonic oscillator, *J.Nonlinear Optical Phys. and Materials* **23** (2014) 1450052-66.

[3] S. S. Hassan, R. A. Alharbey and T. Jarad, Transient spectrum of pulsed-driven harmonic oscillator: damping and pulse shape effects, *Nonlinear Optics and Quantum Optics* **48**(2018) 277-288.

[4] S. S. Hassan R. A. Alharbey and G. Matar, Haar wavelet Spectrum of $\sin^2$-pulsed driven harmonic oscillator, *Nonlinear Optics and Quantum Optics* **48** (2016) 29-39.

[5] S.S. Hassan, G.P. Hildred, R.R. Puri and R.K. Bullough, Incoherently driven Dicke model, *1982 J. Phys. B* **15** (1982) 2635-55.

[6] M.R. Wahiddin, S.S. Hassan and R.K. Bullough, Cooperative atomic behaviour and oscillator formation in a squeezed vacuum, *J. Modern Optics* **42** (1995) 171-189.

[7] L. C. Andrews (1998)," Special functions of mathematics for engineers", (Oxford, Univ. Press, Oxford), 2nd ed.

[8] T. V. Gevorgyan, A. R. Shahinyan, and G. Yu. Kryuchkyan, Generation of Fock states and qubits in periodically pulsed nonlinear oscillators, *Phys. Rev. A* **85** (2012), 053802.

[9] J. Claudon, A. Zazunov, F. W. J. Hekking, and O. Buisson, Rabi-like oscillations of an anharmonic oscillator: Classical versus quantum interpretation, *Phys. Rev. B* **78** (2008) 184503.